

Quantifying chaotic responses of mechanical systems with backlash component

Tegoeh Tjahjowidodo*, Farid Al-Bender, Hendrik Van Brussel

Mechanical Engineering Department, Division PMA, Katholieke Universiteit Leuven, Celestijnenlaan 300B, B3001 Heverlee, Belgium

Received 9 June 2005; received in revised form 4 October 2005; accepted 7 November 2005

Available online 15 December 2005

Abstract

This paper presents a detailed numerical and experimental study of a mechanical system comprising a backlash element that shows chaotic behaviour in a certain excitation range. It aims to quantify the chaotic behaviour of the responses and correlate the quantification parameters to the parameters of the (non-linear) system, in particular the backlash size. The motivation for this investigation is to be able ultimately to identify the parameters of non-linear systems without necessarily being able to ensure periodic behaviour. Application of surrogate data tests is utilised to prove the presence of the chaotic behaviour in the response. The *Simple Non-linear Noise Reduction* is applied to the resulting data to have a better interpretation of the chaotic in the response.

© 2005 Elsevier Ltd. All rights reserved.

Keywords: Backlash; Chaotic; Surrogate data test; Noise reduction

1. Introduction

When excited by a periodic input, a non-linear system may exhibit two types of steady-state response behaviour: periodic or non-periodic, i.e. chaotic. In case of a periodic response, various techniques are available for the characterisation of non-linear systems. Volterra and Wiener series [1] are very suitable for systems exhibiting superharmonic response, while other techniques taken as an extension of linear ARMA theory, namely NARMA and NARMAX have also been developed and proposed for the purpose of identification of various systems [1,2]. The application of the Hilbert Transform (HT) can be effective for practical analysis of the system parameter identification [3–6] for the case of the system with geometric non-linearities. Wavelet analysis was in particular shown to be another identification approach, which offers significant improvement in comparison with HT technique, though it suffers from memory hunger and processing time [5,7].

“Well-behavedness” of a non-linear system is however not always guaranteed, so that under certain excitation conditions, which are not always under our control, chaotic behaviour might occur, rendering the aforementioned techniques inapplicable. In order to be able to deal with such cases, new methods are needed

*Corresponding author. Tel.: +32 16 322515; fax: +32 16 322987.

E-mail address: tgoeh.tjahjowidodo@mech.kuleuven.be (T. Tjahjowidodo).

initially to ascertain if the given behaviour is chaotic and subsequently to characterise the dynamics (e.g. identify certain system parameters) in that regime.

Lin [8] found that a simple mass-spring-damper system comprising a backlash element will show chaotic response under certain excitation conditions. He also demonstrated this behaviour in a supported beam with a mass at its midpoint. Backlash non-linearity was introduced by providing motion constraints on both sides of the mass. However, he did not present chaos quantifiers in order to correlate the model parameters of his system. Theodossiades and Natsiavas [9] showed the chaotic responses in a more complex system, namely a gear pair system with backlash and periodic stiffness. Feng and Pfeiffer [10] studied the chaotic response on a model of a rattling system and presented the bifurcation diagram of the chaotic behaviour as a function of excitation frequency and amplitude. Trendafilova and Van Brussel [11] tried to exploit the chaos quantifiers for fault detection in a real robot joint. They used the high-frequency component of the response besides the excitation frequency to quantify the chaoticity, and correlate it with the backlash size in the robot joint. However, the route of chaos in this high-frequency component signal was not explained.

In the first place, this paper attempts to correlate the chaos quantifiers (namely Lyapunov exponent (λ) and Correlation Dimension), with the parameters of a chaotic system, in particular, for our case, the backlash size. Such correlation methodology could be further developed so as to deal with other non-linear systems such as defect qualification and quantification. Early damage detection in a mechanical system is another possibility to exploit the model. Subsequently, this paper experimentally confirms the possible presence of chaotic response in a real mechanical system with backlash and characterises it.

For the experimental part of this investigation, a robot joint mechanism incorporating a backlash component developed at KULeuven/PMA was used. The experimental set-up consists of a link mechanism, which is driven by a d.c. motor as shown in Fig. 1. Rotation input from the d.c. motor is reduced by a harmonic drive. In this set-up, backlash was introduced in the connection of the harmonic drive to the shaft. Under certain operational conditions, the corresponding mechanism shows chaotic vibration response. However, it is not immediately clear if noise (stochastic process) is not the cause for the aperiodic behaviour. In order to verify this, first we have to recover the embedding dimension of the space and the time lag of the signal for calculating the chaotic quantifications (Lyapunov exponent and Correlation Dimension). Afterwards, a surrogate data test is used in order to check the hypotheses for the presence of chaotic behaviour in the non-linear system and of the linearly correlated noise [11–13]. Once we are convinced that the chaotic process dominates the signal, we have to separate the true response from the measurement noise. For

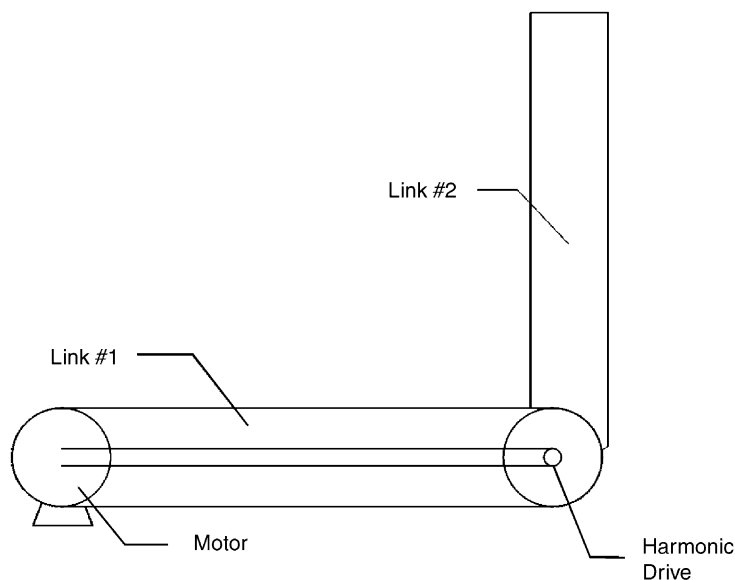


Fig. 1. Schematic illustration of two-link robot manipulator. The first link was kept fixed and two different incremental encoders were used to measure the displacement input from the motor and the displacement output of link #2.

this purpose a simple non-linear noise reduction method (based on the simple non-linear prediction algorithm [14,15]), which is more suitable for chaotic signals, is employed for the recorded signal.

In the following, Section 2 discusses the theoretical treatment of the system under consideration. Section 3 discusses the phase-space reconstruction method and the simulation results, while Section 4 describes a method to detect the presence of the non-linearities and chaotic behaviour on statistical basis including the simulation results. In Section 5, we discuss the implementation of the noise reduction procedure. Thereafter, the experimental set-up and analysis of the data will be presented in Section 6. Finally, some appropriate conclusions are drawn in Section 7.

2. Theoretical basis

Lin [8] shows theoretically that under certain excitation conditions (amplitude and frequency), a simple non-linear mechanical system with backlash shall manifest chaotic vibration. He demonstrates that a simple system comprising a backlash spring, as shown in Fig. 2, and having a dynamic equation:

$$m\ddot{x} + c\dot{x} + k_1x + F(x) = A \cos(\omega t), \tag{1}$$

where $F(x)$ is the restoring force of the non-linear backlash component:

$$F(x) = \begin{cases} k_0(x - x_0), & x \geq x_0 \\ 0, & |x| < x_0 \\ k_0(x + x_0), & x \leq -x_0 \end{cases}$$

is found to behave chaotically under certain excitation conditions. Table 1 gives three sets of the system’s parameters pertaining to chaotic behaviour, for certain excitation force specifications, where m is the mass of the system, k_1 and k_0 are stiffnesses, c is a damping coefficient, and x_0 the backlash (or play) size.

It can be shown that there exist certain sinusoidal excitation forces for Case 1, with $A = 100$ N and for Case 2 with $A = 240$ N, both at $\omega = 40$ rad/s, which cause the response to behave chaotically as shown in Fig. 3. Fig. 4 shows the response of the third case, when the system is excited by a periodic signal with 108 N of amplitude and 1.57 Hz of fundamental frequency. The left panel shows the phase plot of the response in the space of velocity against displacement, while the right panel represents the phase plot in the space of displacement with different time delay.

In order to examine the influence of each parameter on the nature of the resulting response, we use dimensional analysis to normalise the variables and so reduce the number of parameters, making the problem more tractable. Moreover, by combining variables in dimensionless groups, one may gain more insight in the problem.

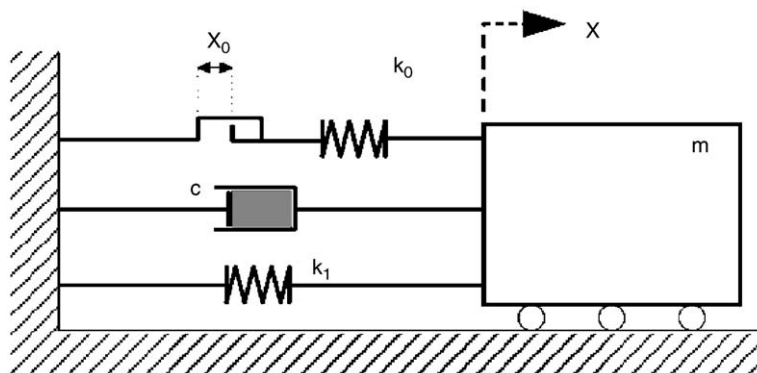


Fig. 2. Schematic of a non-linear mechanical system with backlash component. The system consists of a mass m , a piecewise linear spring component with a stiffness, of k_1 for $|x| \leq x_0$ and $k_0 + k_1$ for $|x| > x_0$, and damping c .

Table 1
Parameter sets of vibration system

	m (kg)	k_1 (N/m)	k_0 (N/m)	c (Ns/m)	x_0 (m)
Case 1	1	0	40000	8	0.005
Case 2	1	1000	31000	8	0.005
Case 3	3	0	2250	8	0.02

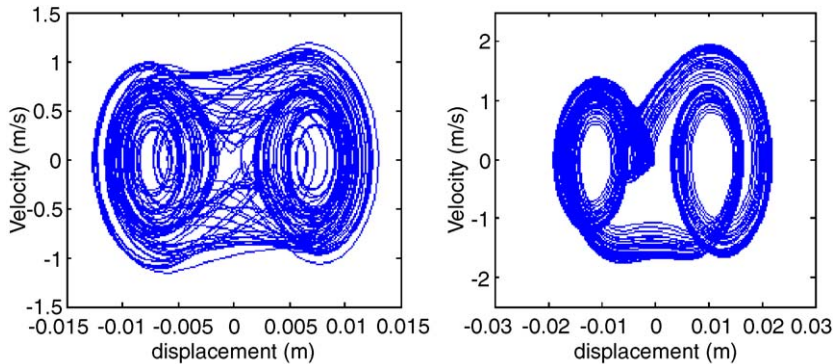


Fig. 3. Phase plots of the chaotic response of two different mechanical systems with backlash component under certain conditions. The left panel shows the phase plot of the response in Case #1 and the right panel for the Case #2.

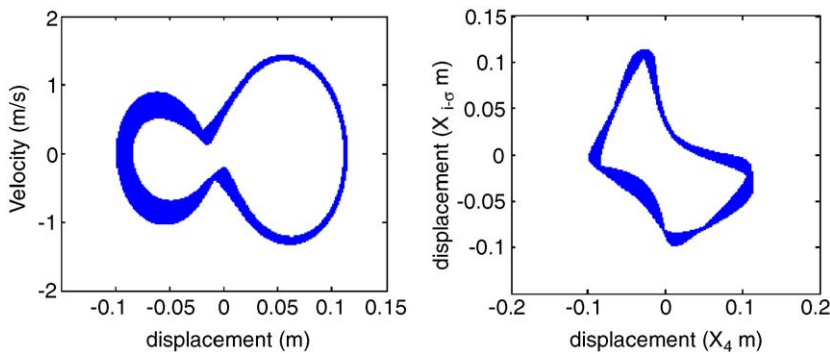


Fig. 4. Phase plots of the chaotic response of Case #3, when the system is excited with sinusoidal signal of 108 N amplitude and 1.57 Hz frequency. The left panel shows the phase plot of the response in the space of velocity against displacement, while the right panel represents the phase plot in the space of displacement with a time delay of 0.102 s, obtained using Mutual Information method.

Introducing new variables of time and displacement $\bar{t} = \omega_0 t$ and $p = x/x_0$, where $\omega_0^2 = k_0/m$, we may rewrite the dynamics equation for Case 1 ($k_1 = 0$) as follows:

$$m\omega_0^2 x_0 p'' + c\omega_0 x_0 p' + k_0 x_0 \bar{F}(p) = A \cos(\omega t), \tag{2}$$

where the primes indicate differentiation with respect to \bar{t} and \bar{F} is the backlash spring function. This equation reduces to

$$p'' + 2\zeta p' + \bar{F}(p) = \alpha \cos \frac{\omega}{\omega_0} \bar{t}, \tag{3}$$

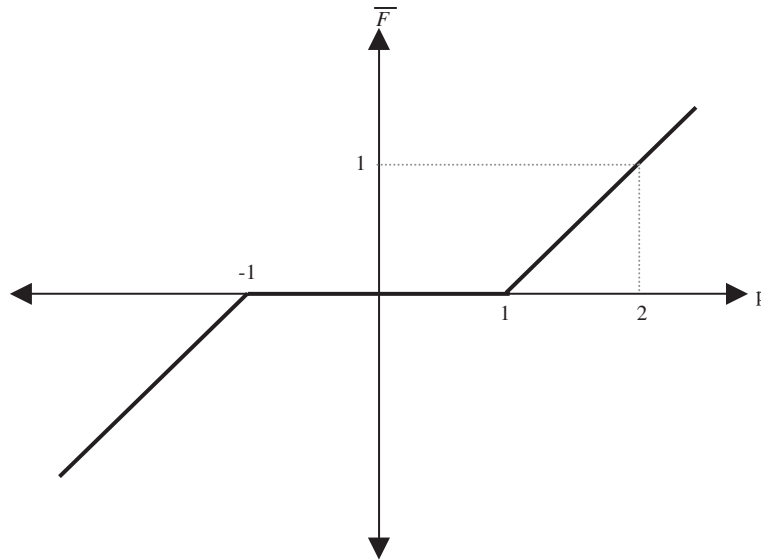


Fig. 5. Force displacement relationship of backlash spring in normalised variables. For $|p| \leq 1$ the spring loses the stiffness and for $|p| > 1$ the stiffness is equal to 1.

where $2\zeta = c/\sqrt{k_0m}$, $\alpha = A/k_0x_0$ and $\bar{F}(p)$ is backlash stiffness characteristic in normalised form:

$$\bar{F}(p) = \begin{cases} (p - 1), & p \geq 1 \\ 0, & |p| < 1 \\ (p + 1), & p \leq -1 \end{cases}$$

as shown in Fig. 5. That is to say that the problem is characterised by two parameters, α (as a function of A , k_0 and x_0) and ζ (function of c , k_0 and m). Let us emphasise that this formulation shows that the dimensionless damping coefficient, ζ , can be varied by varying any or all of the dimensional parameters, c , k_0 or m . Likewise, α can be varied by varying A , k_0 and x_0 . Evidently, varying k_0 will cause a variation in ζ and α simultaneously.

As for the chaos measure, we calculate the maximum Lyapunov exponent of the resulting response. This is based on a unique property of chaotic behaviour that two trajectories starting very close together will rapidly diverge from each other. The divergence (or convergence) of two neighbouring trajectories can be used as a chaos quantification measure, which is the Lyapunov Exponent (λ).

Let us consider two initial conditions in a space p_0 and $p_0 + \delta_0$, each of which will generate an orbit in the space using system equations. These orbits can be thought of as parametric functions of a variable (in general considered to be time). If we use one of the orbits as a reference orbit, then the separation between the two orbits will also be a function of time (δ_t).

In a system with attracting fixed points, δ_t diminishes asymptotically with time. But for a chaotic system, the separation between two trajectories will diverge exponentially fast; hence δ_t will be an exponential function of time:

$$\delta_t = \delta_0 e^{\lambda t}; \lambda > 0. \tag{4}$$

In order to see how a chaotic motion evolves when the forcing amplitude decreases (or equivalently the backlash size or k_0 decrease), we generate a relationship between the largest Lyapunov Exponential (λ) and the parameter $1/\alpha$ for Case 1; Fig. 6 presents the results, which are obtained by simulating the system using Matlab and calculating the Lyapunov exponent by using the TSTOOL toolbox package developed by the *Third Physical Institute, University of Göttingen* [16]. The simulation was carried out repetitively while varying the parameter, in this case $1/\alpha$. For each parameter value, the Lyapunov exponent (λ) was calculated. If the signal is periodic, it yields zero or very low λ . We can set $\varepsilon \rightarrow 0^+$, in such a way that if $\lambda < \varepsilon$, then the resulting λ is set to zero. In some cases it is also possible that the calculation gives positive λ , even when the signal is periodic,

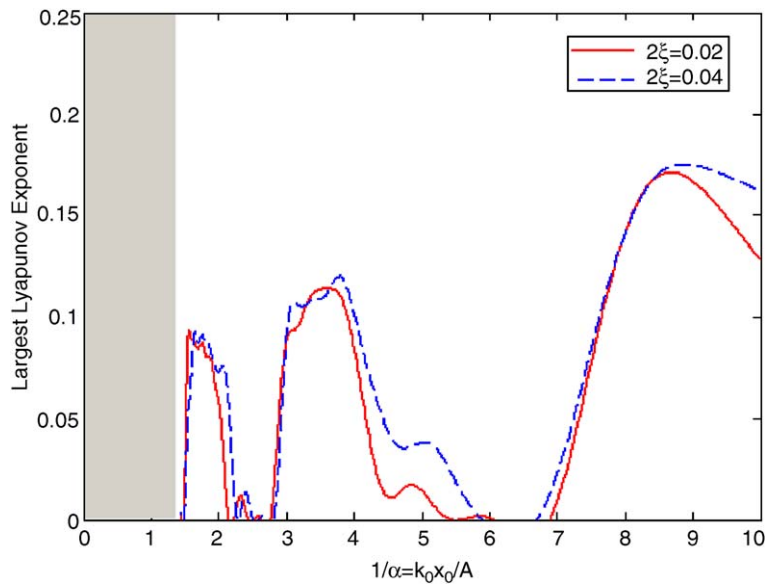


Fig. 6. Largest Lyapunov Exponent vs. $1/\alpha$ for a simple mechanical system with backlash for Case #1. The regions where the Lyapunov exponents are positive indicate the presence of the chaotic response. The Lyapunov exponents in this plot are measured for $1/\alpha \geq 1$.

for instance if the signal is periodic with a very low frequency. However, the separation of two trajectories in terms of Lyapunov exponent, δ_t (see Eq. (4)), might not saturate into a certain value. In that case, we have to reject the positive value of λ .

Fig. 7 shows the corresponding bifurcation diagram, for different damping ratios (ζ) starting from $2\zeta = 0.005$ until $2\zeta = 0.32$. One can conclude from the figure the commonly accepted result that the introduction of higher damping levels is an effective way to diminish and eliminate chaotic motion (the fourth panel of Fig. 7 provides similar representation to Fig. 6 for $2\zeta = 0.04$).

Fig. 8 shows the phase plots of the response of the corresponding mechanical system under different conditions. The top left panel shows the phase plot of the system when $1/\alpha$ is equal to 2.0. Referring to Fig. 6, this system has a positive Lyapunov exponent of approximately 0.06 bit/time, which means that the response is chaotic, resulting in the irregularity of the phase plot in the figure. In contrast, the top right plot of Fig. 8 shows the response of the system when $1/\alpha$ is equal to 2.6. Under this condition, the system clearly has a periodic response, and the non-positive value of the Lyapunov exponent (λ) is consistent with this behaviour. The bottom plots on the same figure show the phase plot of the response under different values of $1/\alpha$ but the same λ . Under different excitation condition ($1/\alpha$), even with the same λ , the responses reveal different fractal structures. The fractal pattern of the corresponding Poincaré maps in Fig. 9 give rigorous evidence that the responses (except those corresponding to the non-chaotic case) are indeed non-periodic and, thus, chaotic.

Recalling Eq. (2), where the dynamic problem is characterised by two parameters, α and ζ , we then need to correlate the effect of both parameters on the chaos quantification. Fig. 10 shows the relation of λ with parameters α and ζ in contour plot. These results confirm the fact that the introduction of higher damping levels is an effective way to diminish and eventually eliminate the chaotic motion. At high damping, there is almost no chaotic response since the λ 's are very low for any value of $1/\alpha$.

Once we have the Lyapunov exponent map as shown in Fig. 10, conceptually, we can estimate the parameters, x_0 and ζ , by observing the evolution of the chaotic response as the system is excited by certain sets of sinusoidal signals with different excitation level at fixed frequency. Assuming that the damping value remains constant for any set of experiments, we can correlate the evolution of the chaotic behaviour in $1/\alpha$ to the parameters, x_0 and ζ , by observing the evolution of λ as a function of $1/\alpha$ similar to that of Fig. 6. Based on Fig. 10, a different degree of backlash will expand (or contract) the range of λ as a function of $1/\alpha$, while the changes of the damping value (ζ) will alter its profile (or shape).

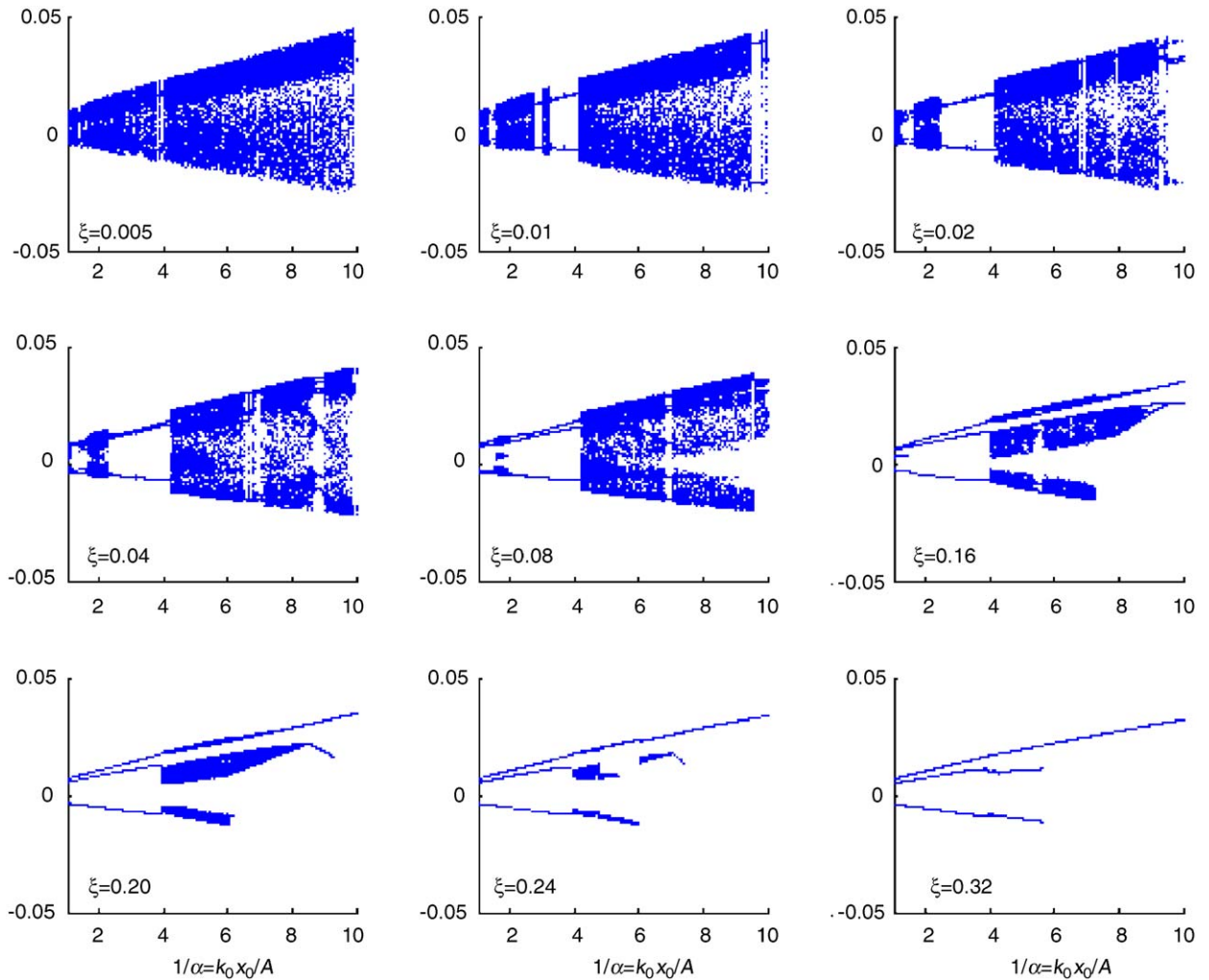


Fig. 7. Bifurcation diagram of a simple mechanical system with backlash for Case #1 for several values of damping. The infinite number of amplitudes marks the existence of the chaotic responses in the system and relate to the positive value of the Lyapunov exponent.

3. Phase-space reconstruction

For a system whose equations of motion are explicitly known, there are some straightforward techniques for computing the chaos quantifiers (namely the maximum Lyapunov exponent and the correlation dimension). The easiest way to obtain the Lyapunov exponent, for instance, is by observing the separation of two close initial trajectories on the attractor. Taking the logarithm of the separation and calculating its slope in time, we can obtain the Lyapunov Exponent. But unfortunately this method cannot be applied directly to experimental data for the reason that we are not always dealing with two (or more) sets of experimental data that have close initial conditions.

Experimental data typically consist of single observable discrete measurements. Reconstructing the phase space from the time series with appropriate time delay and embedding dimension makes it possible to obtain an attractor whose Lyapunov spectrum is identical to that of the original attractor. Mathematically, a reconstructed phase space can be described as follows [14,17]:

$$y(k) = [S(k), S(k + t), S(k + 2t), \dots, S(k + (d - 1)\tau)], \tag{5}$$

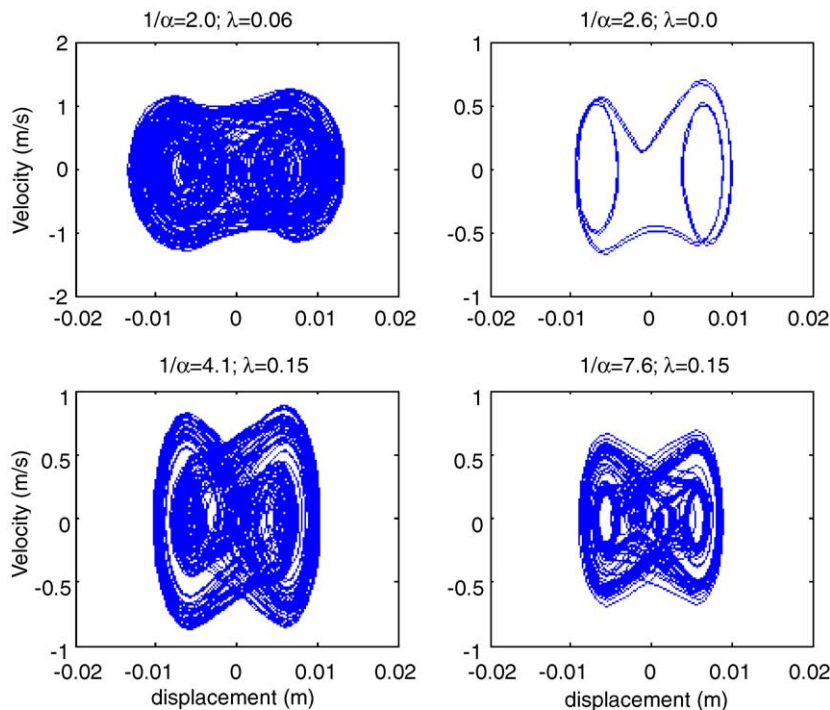


Fig. 8. Phase-plot: projection of trajectories onto (x, x') plane. Top left panel shows the phase plot for the system with $1/\alpha = 2$. Top right panel shows the plot for system with $1/\alpha = 2.6$ that has a periodic response (no chaotic response). Bottom panels show the system with $1/\alpha = 4.1$ and $1/\alpha = 7.6$, which have the same Lyapunov exponent, respectively.

where $S(k)$ is the time series from a single observation, τ represents appropriate time delay for phase-space reconstruction and d is a proper embedding dimension for phase-space reconstruction.

In theory, the largest Lyapunov exponent, λ_1 , is estimated by observing the long-term evolution of a single pair of nearby orbits. The reconstructed phase space, however, contains just one trajectory obtained from experimental data. Nevertheless, if we choose two points in the reconstructed phase space whose temporal separation in the original time series is at least one ‘orbital period’, they may be considered as different trajectories on the attractor.

Hence, the next step in determining the largest Lyapunov exponent for single observable time series is searching the nearest neighbour of certain points, in the sense of Euclidean distance, which can be considered as fiducial trajectories.

3.1. Determining time delay

In a phase-space reconstruction procedure, we must ensure that the points in each dimension (coordinate) are independent of each other. Therefore, time delay τ must be chosen so as to result in points that are not correlated to previously generated points. Analogically, the time delay τ may be considered as time at which the auto-correlation function attains zero. However, the auto-correlation function measures rather the linear dependence between successive points and may not be appropriate when we are dealing with non-linear dynamics. Instead of using the auto-correlation function, the *Average Mutual Information* (AMI) technique can be used for determining appropriate time delay parameter for non-linear time series. Abarbanel [18] suggested that the value of τ for which the first local minimum of the AMI occurs should be taken as time delay, and this is analogous to the time delay when the auto-correlation function attains zero value in linear case.

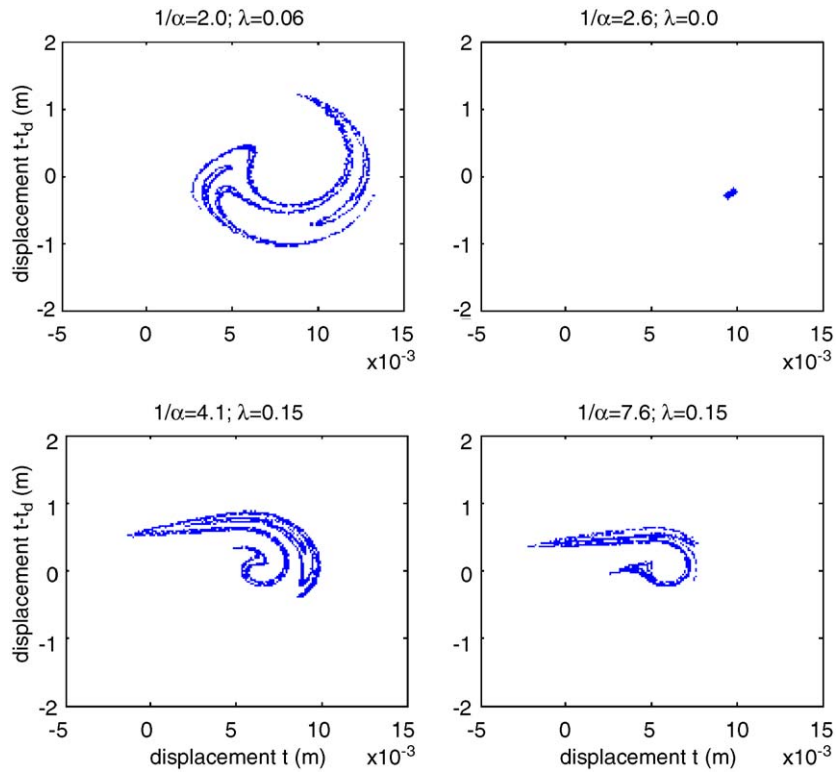


Fig. 9. Poincaré map of different trajectories. Top left panel shows the Poincaré map for the mechanical system with backlash with $1/\alpha = 2$. Top right panel shows the map for system with $1/\alpha = 2.6$ that gives periodic response (no chaotic response). Bottom panels show the system with $1/\alpha = 4.1$ and 7.6 , which have the same Lyapunov exponent, respectively. The plots are constructed using time delay of 0.01 s and calculated using the Mutual Information method.

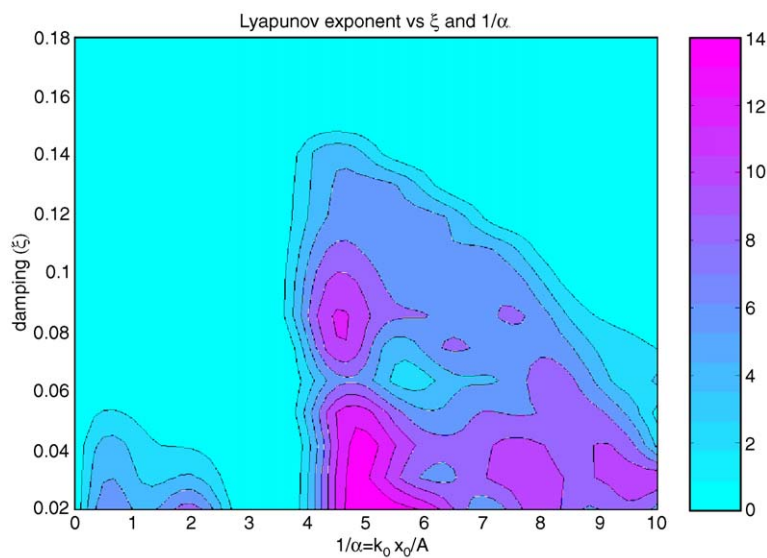


Fig. 10. Lyapunov exponent as a function of two parameters, ξ and $1/\alpha$. A different degree of backlash will expand (or contract) the range of λ as a function of $1/\alpha$, while the changes of the damping value (ξ) will alter the profile.

The mutual information for the set of time series $S(t)$ is formulated by [18] as

$$I(t, t + \tau) = \sum_{S(t), S(t+\tau)} P(S(t), S(t + \tau)) \log_2 \frac{P(S(t), S(t + \tau))}{P(S(t)) \cdot P(S(t + \tau))}, \tag{6}$$

where $P(A,B)$ is the joint probability density for set A and B , and $P(A)$ is the individual probability density for set A .

As illustration, the upper panel of Fig. 11 shows the original time history responses without noise from the simulation of Case #3 as discussed in Section 2. The lower panel of the same figure shows the AMI number for the corresponding data for the case without and with additional noise. The noise was simulated using white noise with maximum values of 1%, 5% and 10% of the mean square of the original data. It can be seen in the figure that the additional noise does not change the first local minimum of the mutual information. Instead, it decreases the value of the AMI itself, since the white noise gives more dependencies between successive points. Fig. 12 shows the Poincaré maps of the same data in Fig. 11. The noise obviously distorts the fractal structure of the original data.

3.2. Determining the embedding dimension

The next step in reconstructing phase space is to recover the appropriate number of coordinates d of the phase space. The idea of a number of coordinates d is a dimension in which the geometrical structure of the phase space is completely unfolded.

Let us consider a phase-space reconstruction in arbitrary dimension d with data vectors as shown in Eq. (5). Examining the nearest neighbour in phase space of vector $y(k)$, we will find

$$y^{NN}(k) = [S^{NN}(k), S^{NN}(k + t), S^{NN}(k + 2t), \dots, S^{NN}(k + (d - 1)t)], \tag{7}$$

where the superscript NN indicates the nearest neighbour vector.

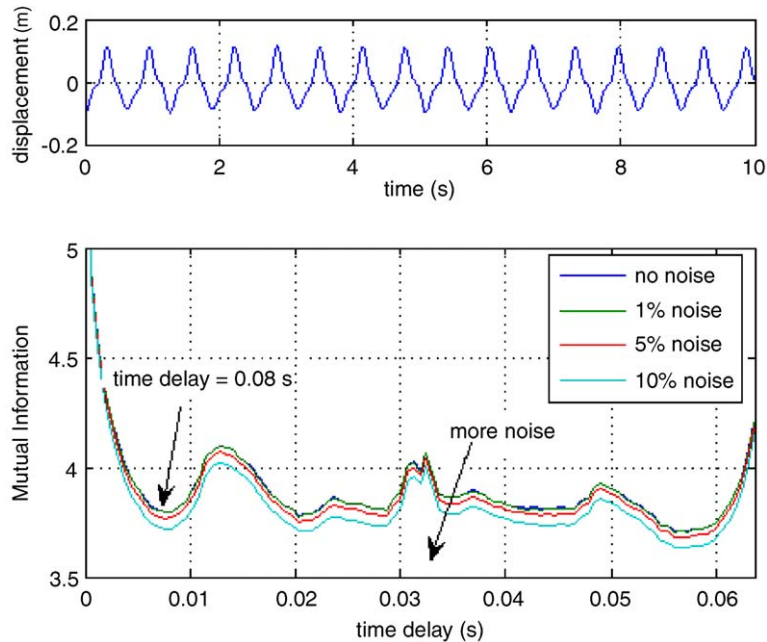


Fig. 11. Time history responses of Case #3 is shown in the upper panel. In the lower panel, the mutual information of the corresponding data can be seen together with the same information for the data with an added white noise of 1%, 5% and 10% of the mean square of the original data.

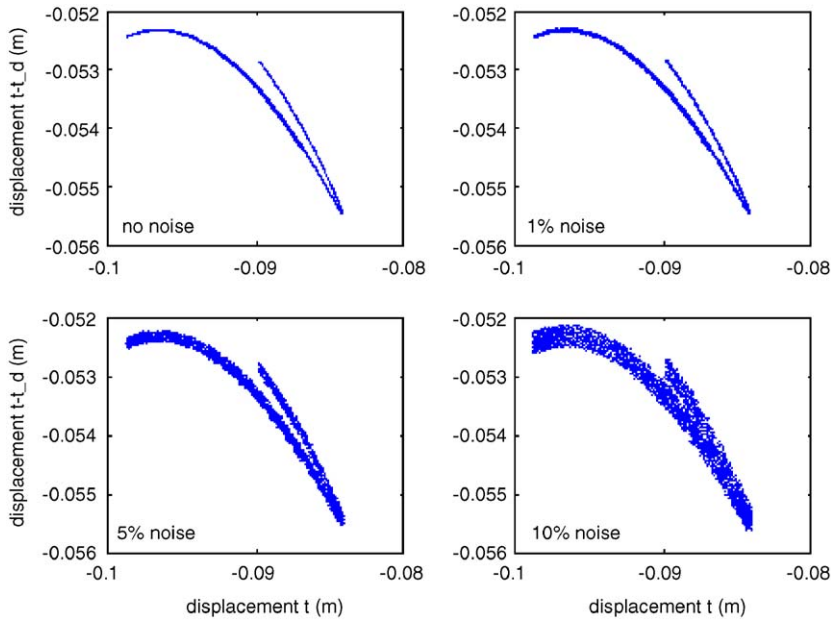


Fig. 12. Poincaré maps of the responses of Case #3. The upper left panel shows the map of the original time series with a time delay of 0.08 s. The upper right, bottom left and bottom right panels show the maps for the cases with noise. The noise distorts the fractal structure of the map.

The basic method in determining the embedding dimension in phase-space reconstruction is the *False Nearest Neighbour* method. Suppose the vector $y^{NN}(k)$ is a false neighbour of $y(k)$, having arrived in its neighbourhood by projection from a higher dimension, because the present dimension d does not unfold the attractor, then by going to the next dimension $d+1$, we may move this false neighbour out of the neighbourhood of $y(k)$.

In going from dimension d to $d+1$, the additional component of the vector $y(k)$ is $S(k+d\tau)$, and the additional component of the vector $y^{NN}(k)$ is $S^{NN}(k+d\tau)$. Comparing the distance between the vectors $y(k)$ and $y^{NN}(k)$ in dimension d with the distance between the same vectors in dimension $d+1$, we can obviously establish which are true neighbours and which are false neighbours. We need to compare the distance $|S(k+d\tau) - S^{NN}(k+d\tau)|$ with the Euclidean distance of $|y(k) - y^{NN}(k)|$ between nearest neighbours in dimension d . If the additional distance is large compared to the distance in dimension d between nearest neighbours, we have a false neighbour. Otherwise, we have a true neighbour.

In order to have a straightforward representation of the minimum embedding dimension, Cao [19] defined the mean value of $a(i,d)$:

$$E(d) = \frac{1}{N-d\tau} \sum_{i=1}^{N-d\tau} a(i,d), \tag{8}$$

where

$$a(i,d) = \frac{R_{d+1}(k)}{R_d(k)},$$

$$\begin{aligned} R_d(k)^2 &= \sum_{m=1}^d [S(k+(d-1)\tau) - S^{NN}(k+(d-1)\tau)]^2 \\ &= R_d(k)^2 + |S(k+d\tau) - S^{NN}(k+d\tau)|^2. \end{aligned}$$

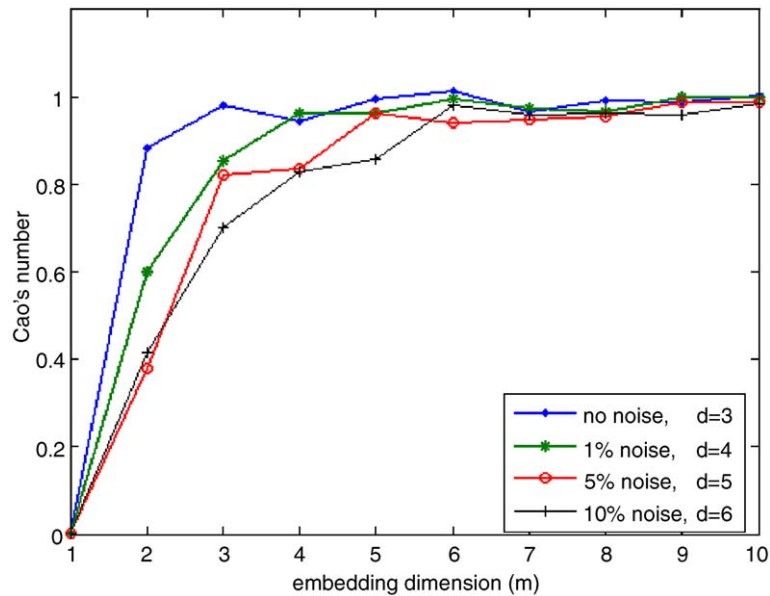


Fig. 13. Minimum embedding dimension of the simulated Case #3 for the cases without and with noise. The noise causes the signal to need more dimensions to completely unfold the attractor.

In order to investigate the variation of $E(d)$ from d to $d+1$, Cao then defined

$$E_1(d) = E(d+1)/E(d). \quad (9)$$

It is easily seen that $E_1(d)$ stops changing when d is greater than some particular value d_0 if the time series comes from an attractor, and its embedding dimension is d_0+1 .

Fig. 13 shows the minimum embedding dimension required by the response in Case #3, which is calculated with Cao's formula. From the figure, we can conclude that the original signal without noise requires at least 3 dimensions to unfold the attractor, since Cao's number approaches a relatively constant value beyond the dimension of 3. The more noise in the signal, the more dimension required to completely unfold the attractor. From the figure, we can see that the signal with 10% of noise requires 6 dimensions to unfold it.

4. Surrogate data testing

Nevertheless, at this stage, it is not clear in any of the cases if noise (linearly stochastic process) is not the cause for the observed irregular behaviour. Surrogate Data Test is utilised to identify whether the behaviour of a signal is caused by the non-linearity in the system or by a random stochastic process. This method first specifies some linear process as a null hypothesis, then generates surrogate data sets, which are consistent with this null hypothesis, and finally computes a discriminating statistics for the original and for each of the surrogate data sets. In order to generate the surrogate data sets, the original data are transformed in such a way that all structures except for the assumed properties are destroyed. The generated surrogate data sets are assumed to mimic only the linear properties of the original data. Theiler et al. [12] state that a Fourier Transform algorithm is very consistent with the hypothesis of linearly correlated noise. This method is achieved by Fourier transforming the original data and substituting the phases with random numbers. After transforming back into the time domain, we get a new time series without affecting the power spectrum. If the discriminating statistic values (namely the maximum Lyapunov exponent, the AMI and/or the correlation dimension) computed for the original data is significantly different from the generated surrogate data, then the null hypothesis is rejected and we conclude that the data is not linearly stochastic noise and the non-linearity is detected.

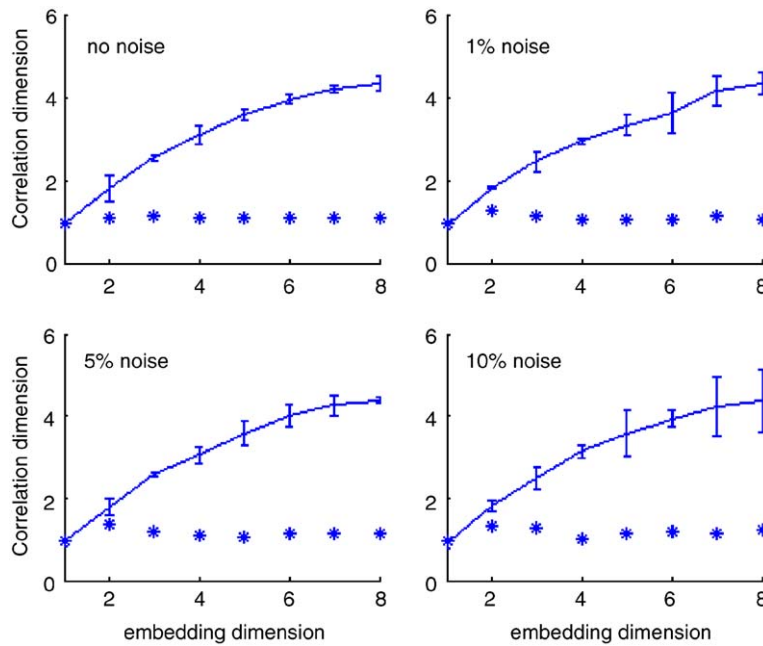


Fig. 14. The correlation dimension of the original data of Case #3 with and without noise and of the surrogates. More noise in the data causes more deviation in the correlation dimensions of the surrogates.

Since we are motivated by the possibility that the underlying dynamics may be chaotic, our original choices for discriminating statistics are the chaotic quantifications. The correlation dimension, D_2 , is the most frequently used as a discriminating statistic in surrogate data test. D_2 is computed as a limit of the correlation sum or the correlation integral [18]:

$$D_2 = \lim_{r \rightarrow 0} \frac{\log |C(2, r)|}{2 \log |r|}, \tag{10}$$

where $C(2,r)$ counts all the points within a distance r of each other.

Generally, if the irregularity in the data is chaotic, going to a higher embedding dimension will not change the result of D_2 . On the contrary, if the data are in fact noise, the correlation dimension will not converge to a specific value in going to a higher embedding dimension.

A theoretical study of the surrogate data testing has been carried out on the same data sets from the previous section, which are used for the theoretical study in the AMI and Cao’s methods. The results of this testing can be seen in Fig. 14. The figure shows the correlation dimension of the original signal (with and without noise) and the average of the surrogates together with the deviations ($3\sigma_x$). From all the panels, we can conclude that the non-linearity is still dominating the signal, since the correlation dimensions of the original signals differ substantially from the surrogates. However, when the data is highly contaminated by noise, the resulting correlation dimensions of the surrogates give higher deviation and the correlation dimensions of the original data are more fluctuating at high embedding dimensions, as can be seen in the bottom right panel of Fig. 14.

5. Noise reduction

A story of an experimental analysis is never complete without discussing the noise reduction step. The noise reduction step plays an important role in estimating the largest Lyapunov exponent to quantify chaotic behaviour. One of the problems in estimating the largest Lyapunov exponent of a ‘noisy’ signal concerns the

minimum embedding dimension required to completely unfold the noisy attractor of the signal. *The Simple Noise Reduction* [15] will be utilised in this work, since it offers superiority, in the calculation time, and simplicity.

The Simple Noise Reduction techniques are closely related to the future prediction theory. For prediction we have no information about the quantity to be forecast other than the preceding measurement, while for noise reduction we have a noisy measurement to start with and we have the future values. Hence we aim to replace the noisy measurement with a set of ‘predicted values’ containing errors, which are on average less than the initial amplitude of the noise.

Suppose the time evolution of our observation is following a deterministic mapping function F : $x_{n+1} = F(x_n)$, which is not known to us. However, our measurement data (s_n) are contaminated by noise:

$$s_n = x_n + \eta_n, \quad (11)$$

where η_n is random noise with no correlation with signal x_n .

The noise reduction scheme is implemented as follows [15]: First, an embedding dimension m has to be chosen by using any method, such as False Nearest Neighbour. Using this information, we can construct an m -dimensional measurement signal $\{s_n\}$. Then for each embedding vector $\{s_n\}$, a neighbourhood $\{U_\varepsilon\}$ is formed and we may determine those which are close to s_n , let us say they are $\{s_n'\}$.

For each embedding vector $\{s_n\}$ a corrected middle coordinate $s_{n-m/2}$ is computed by averaging over the neighbourhood. The reason for using the middle coordinate in this data reduction method is related to the fact that the middle coordinate is assumed to be the most stable direction in a chaotic trajectory.

As an illustration, the noise reduction technique was implemented on the same simulated data of Case #3, and the results are depicted in Figs. 15 and 16. The upper left panel of Fig. 15 shows the Poincaré map of the simulated data without noise and from upper right, bottom left to bottom right we can see the results of the noise reduction process for the data with 1%, 5% and 10% noise, respectively. Fig. 16 shows the zoomed-view of the plots in the corresponding windows. From the figures, we can conclude that the *Simple Noise Reduction* technique performs satisfactorily for the case of the data contaminated by less than 10% noise.

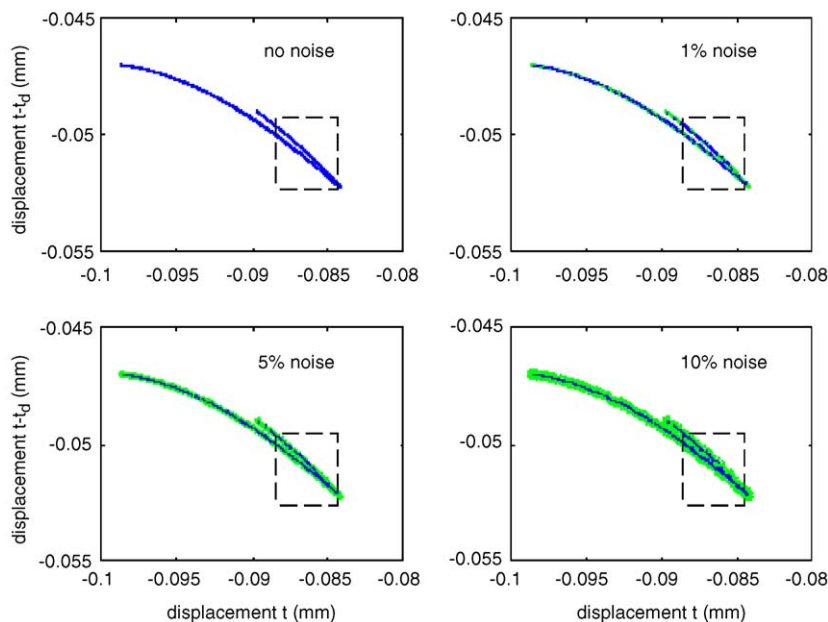


Fig. 15. The Poincaré maps of the simulated data of Case #3 for the cases without and with noise. The lighter dots represent the uncleaned signal.

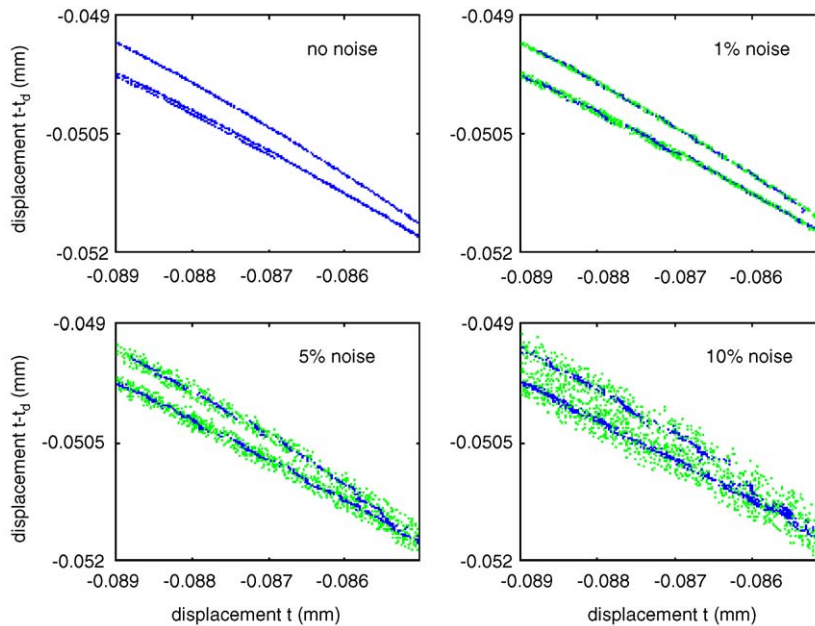


Fig. 16. The magnification of the Poincaré maps of the simulated data. The Simple Noise Reduction method performs well to filter the data which is contaminated less than 10% noise. The lighter dots represent the uncleaned signals.

6. Experimental study

An experiment was carried out on the outer (second) link of a two-link robot manipulator as shown schematically in Fig. 1. The aim of this experiment is to identify the backlash size of the second link joint when chaotic behaviour ensues (the case of periodic response is treated in [6]). For this purpose, a certain degree of backlash (approximately 1.5°) was introduced in the joint of this link. The first link was kept fixed while the second one was made to oscillate over a certain range. This link was driven by a servomotor through a toothed belt and a harmonic drive. The vibration responses were measured by two rotary encoders. The first encoder measured the angular motion input to the harmonic drive, and the second one measured the relative oscillation between the first link and the second link.

Under large amplitude excitation by a periodic force, it is found that the link system shows aperiodic behaviour as can be observed from Fig. 17. The upper panels show the displacement input and output, where the output shows the aperiodicity, while the lower figures show the output after the removal of the fundamental and harmonic frequencies components, in order to emphasise the aperiodicity of the data (subharmonic response is also in evidence). For this case, the system was excited by periodic motion with 1.54 Hz fundamental frequency and amplitude of 2.68° . However, we cannot ascertain whether this aperiodic response is dominated by the presence of linearly correlated noise.

With the aim of having a better understanding on how the chaotic motion arises when the parameters of the system change, in particular the backlash size (as implied by α in dimensional analysis), the experiment was carried out with several different excitation levels ranging from 1.34° to 5.73° , where it was observed that the aperiodic response persisted.

6.1. Determining the time delay

Fig. 18 shows the mutual information of the response shown in the upper right panel of Fig. 17. The first minimum value of the mutual information is approximately 0.174 s. This time delay will be used to reconstruct the phase space of the response in order to measure the Lyapunov exponent. The mutual information will also be used later to check the presence of the non-linearity in the system by using the surrogate data test.

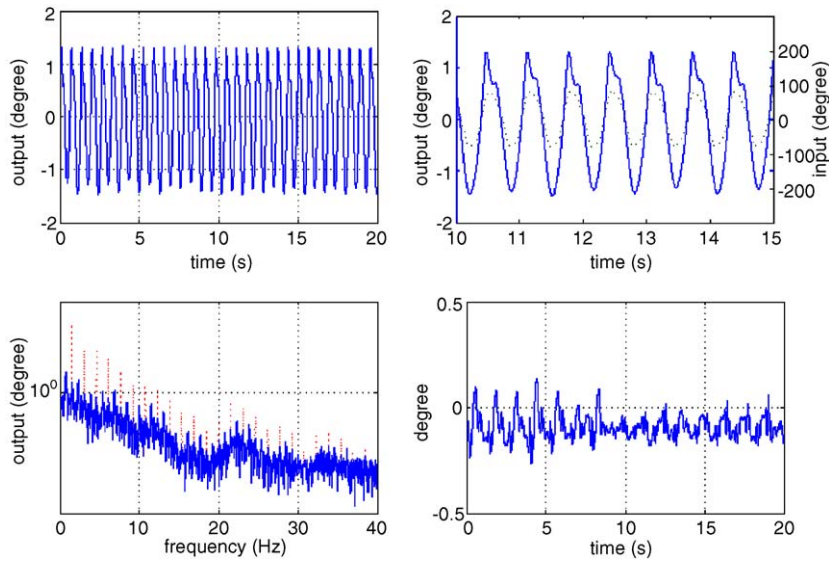


Fig. 17. Output response at 1.54 Hz and 2.68° input excitation. The upper left panel shows the output response while the upper right panel depicts the input and output for selected time windows. The solid line represents the output, while the dashed line is the input. The lower left panel shows the spectra of the output when the harmonic frequency components have been removed (solid line). The dashed line indicates removed component. The bottom right figure shows the inverse Fourier transform of the new spectra.

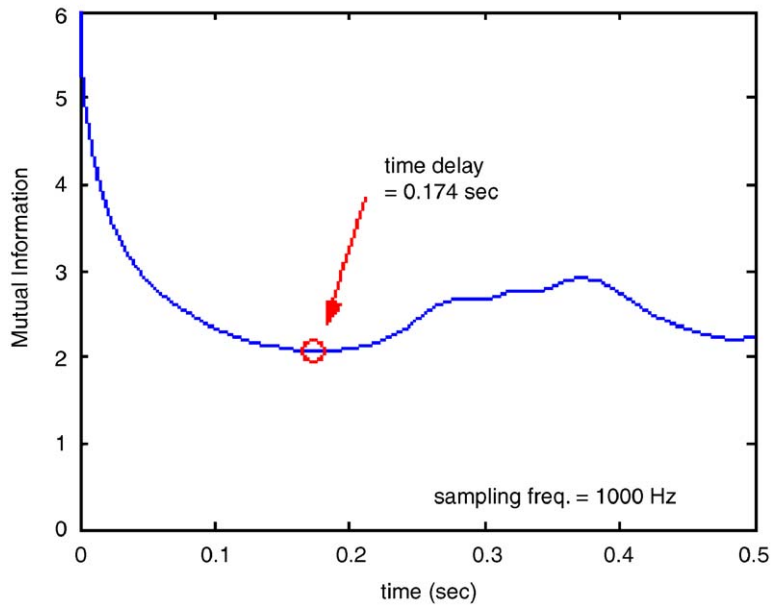


Fig. 18. Average mutual information as a function of the time lag when the system is excited at 2.68° input excitation.

6.2. Determining the embedding dimension

Fig. 19 depicts the Cao’s number as a function of embedding dimension for the experimental case. It can be observed that E_1 approaches a relatively constant value for a dimension higher than 4. Thus, we can conclude that the minimum dimension that will totally unfold the phase space is 5.

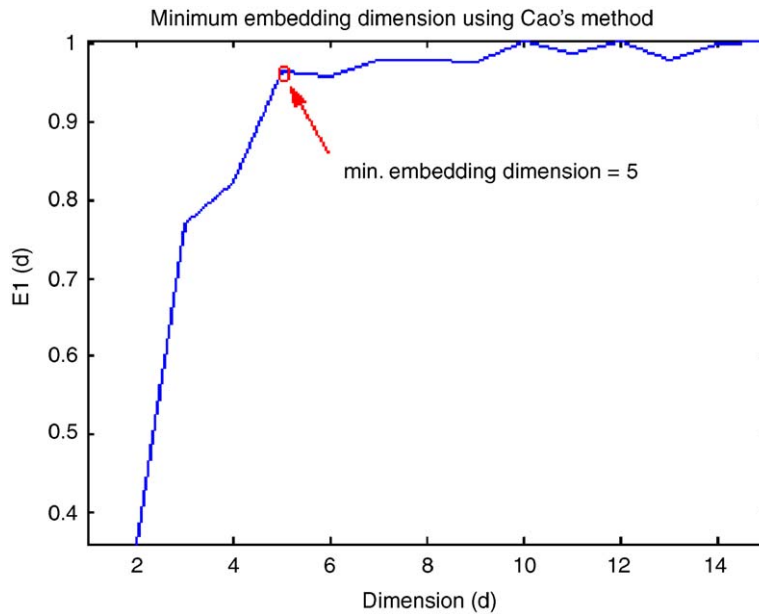


Fig. 19. Minimum embedding dimension when the system is excited at 2.68° input excitation.

Repeating the above sequences for different excitation levels ranging from 1.34° to 5.73° as mentioned before, we obtain the phase-space plots as shown in Fig. 20. The figure shows the phase plots of output responses with certain time delays, which are determined using the AMI method (Section 3.1). Observing the figures, we may suspect that the excitation level of 2.68°, 3.41°, 3.65° and 3.78° result in chaotic responses.

6.3. Surrogate data testing

Fig. 21 shows the plots of the correlation dimension as the discriminating statistics against the embedding dimension, m , for the four suspected chaotic responses of Fig. 20 (excited at levels 2.68°, 3.41°, 3.65° and 3.78°). All of the plots in Fig. 21 show that for all the cases, the values of the correlation dimension for the original data and the surrogates differ substantially. We can also conclude that the figures show the convergences of the correlation dimension for the original data, while the surrogates show no convergences. The estimated dimensions of the original data, about $d = 2.50, 2.10, 1.55$ and 2.10 in ascending excitation level order, respectively, shows that the underlying dynamics is in fact chaotic.

6.4. Maximum Lyapunov exponent in time series

The first step in determining the largest Lyapunov exponent from time series begins by choosing a certain point, say, $y(1)$ in embedding space with dimension of d and time delay of τ (see Eq. (4)). Based on the reconstructed phase space, we can find $y^1(1)$ as the nearest neighbour of $y(1)$, whose temporal separation of both points in the original time series is at least one mean orbital period.

Let us now express the next n time steps $y(1)$ as $y(1,n)$, while $y^1(1,n)$ is the next n time steps of the nearest point $y^1(1)$. Observing the evolution of both points, $y(1)$ and $y^1(1)$, and computing the exponential separation between two trajectories, which are originally coming from single observable trajectory, we can simply define the largest Lyapunov exponent value.

Averaging this value for m neighbours, $y^m(1)$, where the distances to the reference point $y(1)$ are smaller than ε , the exponential separation, which generally varies along the trajectories, will be averaged out.

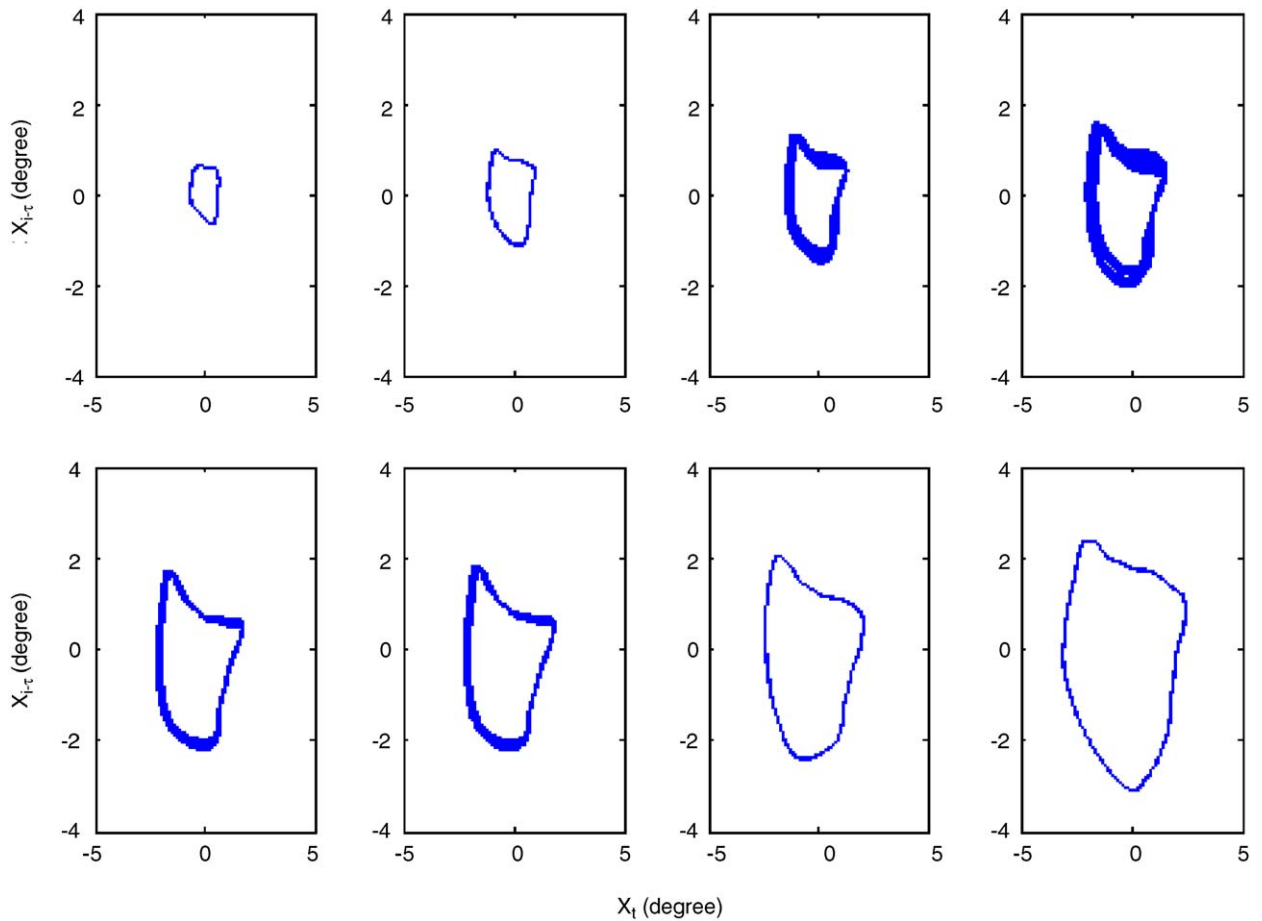


Fig. 20. Phase plots of output responses with certain discrete unit time delay of corresponding mechanical system with excitation frequency of 1.54 Hz and amplitude level, respectively, from left to right and top to bottom: 1.34°; 2.07°; 2.68°; 3.41°; 3.65°; 3.78°; 4.87°; 5.73°.

Table 2 shows the chaos quantification based on Lyapunov exponents for corresponding results in Fig. 20, starting from the lowest excitation level to the highest. The evolution of the Lyapunov exponents as shown in the table obviously marks the bifurcation phenomenon in the system. The response behaves periodically at low excitation levels until it reaches certain level between 2.07° and 2.68°, then the chaotic response grows. Subsequently, after certain excitation level (between 3.78° and 4.87°), the chaotic behaviour diminishes, and the response, again, behaves periodically.

6.5. Noise reduction process

Fig. 22 shows the result of the Simple Noise Reduction method of output response when the system was excited using 3.41° excitation level, compared to the uncleaned one. One may see that the trajectory appears smoother after noise reduction. Verification and quantification of the noise reduction performance can be done on the basis of the correlation integral [14]. For our case, since the noise level is not significantly high, this verification will not be discussed in this paper. The phase plot of this signal is qualitatively not similar to the simulated ones in every detail, since in practice, several mechanical parameters are not considered, such as the friction in the joint of the two-link mechanism.

In Fig. 23, we can see the plot of the Cao's number $E1$ vs. its embedding dimension d . The solid line represents $E1$ for the original noisy signal, while the dashed line represents $E1$ for the signal when its noise has

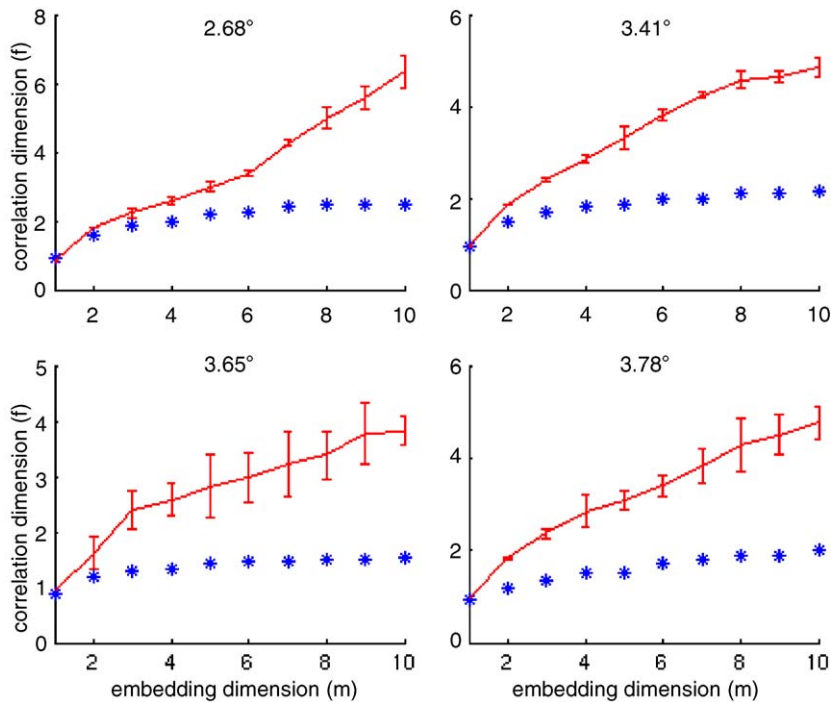


Fig. 21. The correlation dimension vs. embedding dimension for the original data (excited at excitation levels 2.68°, 3.41°, 3.65° and 3.78°) and for the surrogates. The values of the correlation dimension for the original data and for the surrogates differ substantially, and the convergence value of the original data suggests that the underlying dynamics is chaotic.

Table 2
Chaotic quantification results of series excitation

Exc. level	1.34°	2.07°	2.68°	3.41°
Largest Lyap. (bit/time)	—	—	1.423	1.322
Exc. level	3.65°	3.78°	4.87°	5.73°
Largest Lyap. (bit/time)	1.533	1.802	—	—

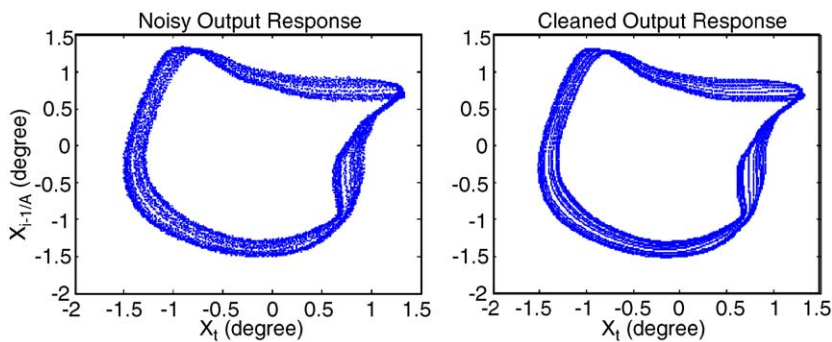


Fig. 22. The cleaned signal compared to the noisy one. The left panel shows the phase plot of the response of the system under excitation frequency of 1.54 Hz and amplitude level of 2.68° before noise reduction, while the cleaned signal can be seen in the right panel.

been reduced. From the figure we can see that the noisy signal needs a higher dimension to unfold its attractor compared to its cleaned counterpart. The noisy one takes a minimum of 5 embedding dimensions to completely unfold its attractor, while the cleaned one needs only 4.

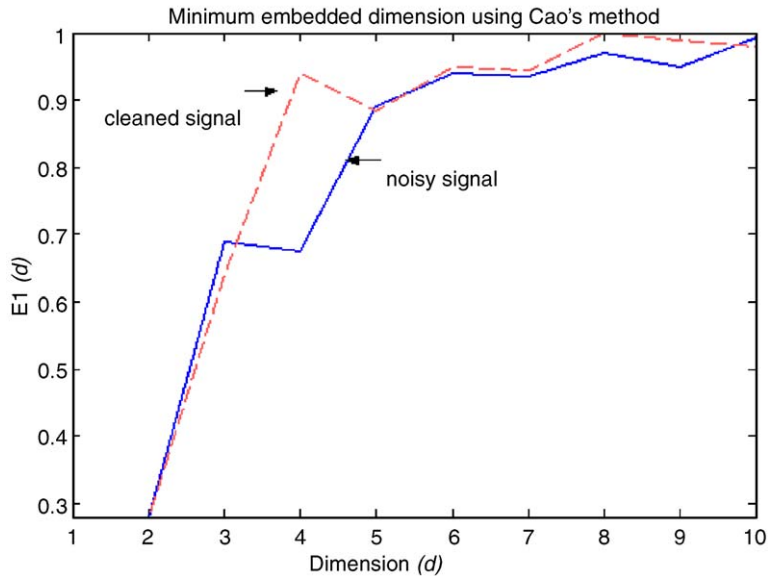


Fig. 23. Estimation of the minimum embedding dimension of noisy and cleaned signals using Cao's method. The noisy signal needs more dimensions to completely unfold the attractor compared to the cleaned one.

7. Conclusion

The following conclusions can be drawn from this investigation:

- Under certain excitation conditions in a non-linear system, there may exist some separate regions for which chaotic vibrations could occur. The transition to and from those regions is marked by bifurcation points. We have shown that, for this case, of a system with backlash, it would be possible to quantify the Lyapunov exponent, for each amplitude of excitation. Correlating the Lyapunov exponent with $\alpha = A/k_0x_0$ could, in principle, yield the backlash size. In some cases, several different backlash sizes could give the same value of Lyapunov exponent. Introducing another quantification concept, namely the correlation dimension, different backlash sizes for the same value of Lyapunov exponent can be distinguished.
- The presence of the chaotic behaviour is confirmed in the surrogate data testing using correlation dimension as the discriminating statistic. The discrepancies of the correlation dimensions between the original data and their surrogates, in some certain excitation conditions, ascertain the presence of the non-linearities in the system. Specifically, the convergence value of the correlation dimension against the embedding dimension proves that the underlying dynamics are chaotic.
- For a simple chaotic system, as gauged by its attractor's dimension, with relatively low noise level, the Simple Noise Reduction method gives very good result. This noise reduction method is therefore very suitable for application to simple systems since it offers superiority in calculation time.

In short, although quite difficult to perform in practice, chaos quantification could be used as a quantitative mechanical signature of a backlash component. Noise reduction plays an important role in this quantification.

Acknowledgements

The authors wish to acknowledge the partial financial support for this study by the Volkswagenstiftung under Grant No. I/76938. The authors are grateful for some critical remarks from the reviewers which have led to improvements in the paper.

References

- [1] K. Wyckaert, Development and evaluation of detection and evaluation schemes for the nonlinear dynamical behaviour of mechanical structures, Ph.D. Thesis, Department of Mechanical Engineering, Division PMA, Katholieke Universiteit Leuven, 1992.
- [2] G. Tomlinson, Detection, identification and quantification of nonlinearity in modal analysis, in: *Proceedings of the Fifth International Modal Analysis Conference*, 1987.
- [3] M. Feldman, Non-linear system vibration analysis using Hilbert transform—I. Free vibration analysis method ‘FreeVib’, *Mechanical Systems and Signal Processing* 8 (2) (1994) 119–127.
- [4] M. Feldman, Non-linear system vibration analysis using Hilbert transform—II. Forced vibration analysis method ‘ForceVib’, *Mechanical Systems and Signal Processing* 8 (3) (1994) 309–318.
- [5] T. Tjahjowidodo, F. Al-Bender, H. Van Brussel, Identification of backlash in mechanical systems, in: *Proceedings of the 2004 ISMA International Conference on Noise and Vibration Engineering*, Leuven, Belgium, 2004, pp. 2195–2209.
- [6] T. Tjahjowidodo, F. Al-Bender, H. Van Brussel, Experimental dynamic identification of backlash using skeleton methods, *Mechanical System and Signal Processing* (2005), in press, doi:10.1016/j.ymssp.2005.11.002.
- [7] W.J. Staszewski, Identification of nonlinear systems using multi-scale ridges and skeletons of the wavelet transform, *Journal of Sound and Vibration* 214 (1998) 639–658.
- [8] R.M. Lin, Identification of the dynamic characteristics of nonlinear structures, Ph.D. Thesis, Mechanical Engineering Department, Imperial College of Science, Technology and Medicine, London, UK, 1990.
- [9] S. Theodossiades, S. Natsiavas, Nonlinear dynamics of gear pair systems with periodic stiffness and backlash, *Journal of Sound and Vibration* 229 (2) (2000) 287–310.
- [10] Q. Feng, F. Pfeiffer, Stochastic model on a rattling system, *Journal of Sound and Vibration* 104 (2) (1998) 328–342.
- [11] I. Trendafilova, H. Van Brussel, Nonlinear dynamics tools for the motion analysis and condition monitoring of robot joints, *Mechanical Systems and Signal Processing* 15 (2001) 1141–1164.
- [12] J. Theiler, S. Eubank, A. Longtin, B. Galdrikian, J. Farmer, Testing for nonlinearity in time series: the method of surrogate data, *Physica* 58D (1992) 77–94.
- [13] T. Shreiber, A. Schmitz, Surrogate Time Series, available online: http://www.mpiyks-dresden.mpg.de/~tisean/TISEAN_2.1/docs/surropaper/Surrogates.html
- [14] A.A. Tsonis, *Chaos: From Theory to Applications*, Plenum Press, New York, 1992.
- [15] H. Kantz, T. Schreiber, *Nonlinear Time Series Analysis*, Cambridge University Press, Cambridge, 1997.
- [16] H. Kantz, T. Schreiber, TSTOOL Homepage, DPI Göttingen, <http://www.physik3.gwdg.de/tstool/>.
- [17] R.C. Hilborn, *Chaos and Nonlinear Dynamics: An Introduction for Scientist and Engineers*, Oxford University Press, Oxford, 1994.
- [18] H. Abarbanel, *Analysis of Observed Chaotic Data*, Springer, Berlin, 1996.
- [19] L. Cao, A. Mees, K. Judd, G. Froyland, Determining the minimum embedding dimensions of input–output time series data, *International Journal of Bifurcation and Chaos* 8 (1997) 1491–1504.